Periodic trends in the geometric structures of 13-atom metal clusters

Yan Sun,[1] Min Zhang,[1] and René Fournier[2]
[1]*Department of Physics, York University, Toronto, Ontario, Canada M3J 1P3*
[2]*Department of Chemistry, York University, Toronto, Ontario, Canada M3J 1P3*
(Received 19 November 2007; published 29 February 2008)

We report structures of X_{13} clusters for 26 metal elements found by global optimization of the energy calculated by density functional theory. The icosahedron is unstable in 19 of those cases. There are at least 11 truly distinct structures among the 26 global minima. Differences in geometries between elements are understood as resulting from competing structural principles. Periodic trends in structure relate to atomic properties. Cagelike features correlate with hardness, $(\mathrm{IE}-\mathrm{EA})/2$, and the number of 90° bond angles correlates with *p*- and *d*-type orbital participations in localized bonds.

DOI: 10.1103/PhysRevB.77.075435 PACS number(s): 61.46.Bc, 36.40.Mr, 31.10.+z

I. INTRODUCTION

Metal clusters X_n have properties that are different from those of the bulk and often vary nonmonotonically with n.[1,2] This makes clusters interesting, but also vexing, because these variations are hard to understand when one does not know the geometric structure. Experimentally, cluster concentrations are very low and ion based techniques are normally used. This is suitable for studying electronic properties but often gives only indirect information about geometric structure. Making inferences about the structure of metal clusters based on a good agreement between experimental and calculated electronic properties and fragmentation energies can be dangerous. If the jellium is a good model for that metal, those electronic properties depend only weakly on nuclear positions and many different cluster geometries can give equally good agreement with experiment.[3] There are few instances where cluster structures have been established with a good degree of confidence; some examples can be found in recent articles.[4,5] More often, properties are rationalized on the basis of hypothetical structures obtained with simple models. Two such models have been used for many years and have special importance: electronic shells (ESs) and atomic shells (ASs).[2]

The ES model, often associated with the ellipsoidal jellium model (EJM), is based on the idea that the electronic wave function symmetry dictates the position of nuclei, at least in an average sense. The EJM accounts for size-dependent variations in stability and ionization potentials for clusters of alkali and few other metals, but makes only vague predictions about structure. It predicts shape as a function of number of delocalized electrons, in particular, "strongly prolate" for 13 and 26 electrons, and "weakly oblate" for 39 electrons.[6]

The idea that surface energy should be minimized, or equivalently, that the number of nearest-neighbor (NN) pairs should be maximized, leads to AS models. Pair potentials, and the embedded atom method and related models, almost invariably maximize the number of NN pairs irrespective of the element or details in parametrization.[7] This leads to polytetrahedral global minima (GM) and shell closing occuring at $n=13$ with the icosahedron (ICO). The 13-atom ICO structure is seen experimentally in rare gas clusters, apparently in some metal clusters, and within the amorphous bulk phase of some elements and alloys.[8]

First-principles methods such as density functional theory (DFT) make no *a priori* assumptions and can in principle make correct structure predictions that would test the validity of ES, AS, and other structural principles. However, finding the GM is hard because there are many local energy minima, likely more than a thousand for X_{13}. So, aside from errors inherent to various implementations of DFT, finding the GM is hard. However, highly efficient search algorithms have been developed recently, for example, taboo search in descriptor space (TSDS),[3,9] which can be combined with DFT for GM prediction. The 13-atom clusters are especially interesting because ICO X_{13} has 42 NN pairs compared to 38 or fewer for other geometries, and is predicted to be very stable ("magic") compared to other structures and sizes in the AS model. Chang and Chou proposed a biplanar fcc fragment structure for X_{13} and showed, by DFT, that it is more stable than the ICO for late second-row transition metal (TM) elements.[10] However, they did not search for GM. Separate DFT studies of various X_{13} metal clusters were done recently, some suggesting an ICO GM[11–13] and others a non-ICO GM.[14–16] Here we report a systematic search for the GM of 13-atom metal clusters for 23 elements shown in Fig. 1, and we also include earlier results for Li,[17] Be,[18] and Al.[3] We made no *a priori* assumption about structure and performed global optimizations of energy evaluated by DFT. To our knowledge, analysis of cluster structures of X_n $(n>6)$ obtained by combined first-principles energy calculations and global optimization has not been done before for more than four elements *X*.[19] As we will show, comparing a large number of GM, all obtained by first principles, brings unique insight into periodic trends and factors that favor some cluster structures.

II. COMPUTATIONAL DETAILS

Many calculations combined global optimization done by TSDS with an energy evaluated with the GAUSSIAN03 software[20] using the local spin density (LSD) approximation and LANL2DZ effective core potential and basis, followed by local optimizations with either a LSD or PBE[21] treatment of exchange correlation (XC) which we denote TSDS-LSD

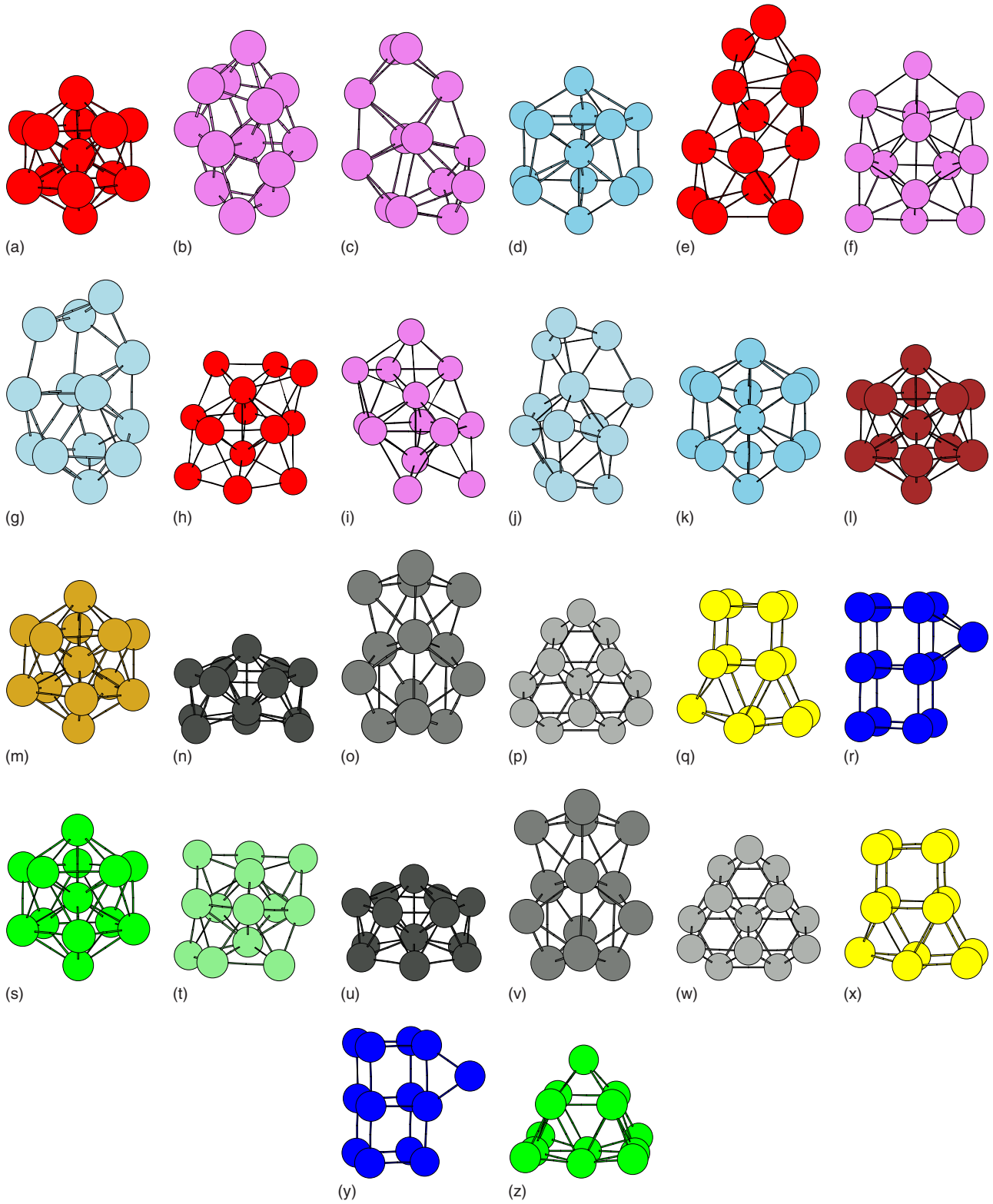

FIG. 1. (Color online) Global minima of 13-atom clusters. (a) Li, (b) Be, (c) Mg, (d) Al, (e) K, (f) Ca, (g) Zn, (h) Rb, (i) Sr, (j) Cd, (k) In, (l) Y, (m) Zr, (n) Nb, (o) Mo, (p) Tc, (q) Ru, (r) Rh, (s) Pd, (t) Ag, (u) Ta, (v) W, (w) Re, (x) Os, (y) Ir, (z) Pt.

and TSDS-LSD/PBE, respectively. In other cases we calculated the energy with the VASP software[22] using the plane-augmented wave method[23] and PBE, and optimized with either simulated annealing (SA-PBE) or TSDS (TSDS-PBE). We also did a few more local optimizations for structures taken from the literature or from results for other elements. Different spin states were tried in each case. Vibrational frequencies were calculated to confirm that each structure is a

TABLE I. Spin magnetic moment ($2S$), relative energy with respect to the icosahedron (RE), number of nearest neighbors (S_{NN}), shape (η), and square (R) descriptors of GM of X_{13} for elements in groups 1, 2, 12, and 13.

	$2S$ (μ_B)	RE		S_{NN}	η	R	
		LSD	PBE				
Li_{13}	5	0.00		42	0.00	0.0	Ref. 17/L
Be_{13}	0	−0.95	−1.02	33	0.35	1.3	Ref. 18/L
Mg_{13}	0	−1.57	−1.41	33	0.49	1.3	TL
Al_{13}	1	−0.45	−0.32	36	−0.05	1.1	Ref. 3/P
K_{13}	0	−0.24	−0.14	35	0.35	0.8	TL
Ca_{13}	0	−0.53	−0.40	38	−0.04	0.0	TL
Zn_{13}	0	−1.03	−0.52	32	0.46	1.5	TL
Rb_{13}	1	−0.39	−0.30	38	−0.01	0.1	TL/P
Sr_{13}	0	0.00	−0.06	38	0.18	0.0	TL/P
Cd_{13}	0	−0.35	0.00	33	0.31	1.4	TL
	0			42	0.00	0.0	TL/P
In_{13}	1	−0.24	−0.28	37	−0.05	1.9	TL/P

minimum. We assigned a tag (last column of Tables I and II) to each GM to indicate how that structure was found. The tag indicates the method we used (T=TSDS, S=SA, L=LSD, and P=PBE), or a literature reference (see, e.g., Rh_{13}), or that another element's GM was used as a trial structure for local optimization (see, e.g., Mo_{13}). We also did calculations with a hybrid (B3LYP) XC functional in a few cases. The structures shown in Fig. 1 (and GM of Cd_{13}), which are the basis for our analysis, were all obtained using the PBE functional in the final local optimization step, except for some of the simpler metals for which we used LSD: Li, Be, Mg, K, Ca, and Zn.

Any discussion of cluster structure is complicated by the fact that there are many cluster isomers, sometimes close in energy to the GM, that may or may not have the same spin state. Different XC functionals can give different GM and energy ordering of cluster isomers.[24] In Sec. III we will show energy differences that are often much too small for us to

TABLE II. Spin magnetic moment ($2S$), relative energy with respect to the icosahedron (RE, in eV), number of nearest neighbors (S_{NN}), shape (η), and square (R) descriptors of GM of X_{13} for transition metal elements.

	$2S$ (μ_B)	RE		S_{NN}	η	R	
		LSD	PBE				
Y_{13}	19	0.00	0.00	42	0.00	0.0	TL/P
Zr_{13}	6	0.00	0.00	42	−0.06	0.1	TL/P
Nb_{13}	1	−0.75	−0.57	37	−0.04	1.1	Ta/P
Mo_{13}	0	−0.05	−0.18	33	0.41	1.8	W/P
Tc_{13}	1	−3.9	−1.84	36	−0.31	2.6	TL/P
Ru_{13}	2	−3.6	−2.59	26	0.19	3.2	SP
Rh_{13}	1	−1.75	−0.72	29	0.19	3.4	Ref. 27/P
Pd_{13}	8	−0.12	0.00	42	−0.05	0.1	TL/P
Ag_{13}	1	−1.38	−0.98	38	−0.04	0.1	TL/P
Ta_{13}	1	−0.53	−0.58	38	−0.06	0.8	SP
W_{13}	0	−2.52	−1.60	35	0.40	1.7	TP
Re_{13}	5	−3.80	−3.89	36	−0.33	2.6	SP
Os_{13}	4	−5.48	−6.22	27	0.18	3.2	SP
Ir_{13}	3	−5.91	−6.49	24	0.11	3.3	SP
Pt_{13}	2	−2.85	−3.31	33	−0.18	1.3	SP

assign the GM with confidence, even theoretically. However, for the purpose of studying periodic trends, we must choose a set of representative structures. We chose to simply take the lowest PBE energy structure for each element. We could instead have chosen to weigh each isomer, for example, using Boltzmann factors like was done in a study on silver clusters.[25] However, this would complicate the analysis and discussion enormously because we typically found 3–10 isomers for each of the 26 cases, and it would not bring any clear benefit for two reasons. First, low-lying cluster isomers often have features similar to the GM in Fig. 1. Second, with so many cases there is often error compensation and some trends are robust. For example, the Pd_{13} ICO is the GM but it is favored by less than 0.01 eV, whereas the Sr_{13} ICO is not the GM but is only 0.06 eV above the GM. Neglecting one of the ICO (Sr_{13}) as we did, or counting both ICO (Pd_{13} and Sr_{13}) each with a weight of 1/2, gives essentially the same conclusion about what fraction of GM are ICO. We will only briefly mention cluster isomers, spin states, and differences between XC functionals: we defer a full discussion of isomerism and properties other than structure to future papers. Here we are concerned with trends and general features found among the lowest energy structures of X_{13}. Considering the difficulty in global optimizations and the unknown errors associated with various functionals, there is no guarantee that the structures in Fig. 1 correspond to real cluster geometries. However, they have low energy and constitute a realistic sample set of possible structures suitable for studying periodic trends. With these caveats in mind, we take the structures in Fig. 1 as the putative GM. In order to characterize the geometries we use descriptors. They are the number of NN pairs S_{NN} defined as

$$S_{NN} = \frac{1}{2}\sum_j c_j \tag{1}$$

where

$$c_j = \sum_{i \neq j} f(d_{ij}/d_0)$$

and

$$f(x) = (1.3 - x)/0.2 \quad \text{when } 1.1 < x < 1.3,$$

$$f(x) = 1 \quad \text{when } x < 1.1,$$

$$f(x) = 0 \quad \text{when } 1.3 < x,$$

and d_0 is the average NN distance in the cluster; the root-mean-square deviation from the mean of atomic coordinations RMSD(c),

$$\mathrm{RMSD}(c) = \left[\frac{1}{13}\sum_{j=1}^{13}(c_j - S_{NN}/6.5)^2\right]^{1/2}; \tag{2}$$

two descriptors that express the asphericity (ζ) and shape (η) of the cluster and which are calculated from the three moments of inertia $I_a > I_b > I_c$,

$$\zeta = \frac{(I_a - I_b)^2 + (I_b - I_c)^2 + (I_c - I_a)^2}{(I_a^2 + I_b^2 + I_c^2)}, \tag{3}$$

$$\eta = (2I_b - I_a - I_c)/I_a; \tag{4}$$

and 1/13 the number of bonds that are at 90°, R,

$$R = \frac{1}{13}\sum_j \sum_{k>\ell} \cos(\theta_{kj\ell} - 90^\circ)^{100} \tag{5}$$

where k and ℓ index the neighbors of atom j. Taking the power 100 is arbitrary; it is just a way to count angles and produce R values that are intuitively meaningful. The overall shape of a cluster is indicated by η as prolate ($\eta > 0$) or oblate ($\eta < 0$).

III. RESULTS AND DISCUSSION

Many structures in Fig. 1 have been proposed before as GM[13,11,14,15,17,18,26,27] based on various kinds of DFT calculations. Our search for Zr and Tc gave GM that had been suggested in earlier studies where global optimization was not done.[10,28] Our GM resemble those previously reported for Ca (Ref. 29) and Ag (Ref. 30) but apparently differ in the positions of a few capping atoms. We report the energy of the GM relative to the ICO in Tables I and II.

Before getting into a discussion of the GM structures, a few comments about higher energy isomers are in order. Isomers close in energy to the GM sometimes change their order with XC functional. For example, the GM is an ICO for Sr_{13} (LSD, B3LYP); the GM of Rh_{13} (B3LYP) is like Re_{13}; the GM of Pd_{13} (LSD) is like Ca_{13} and that isomer is only 0.01 eV above the ICO in PBE; Li_{13} (LSD) has an isomer at +0.05 eV with S_{NN}=37 and η=0.37 which is similar to the GM of K_{13}; and Mo_{13} (PBE) has a non-ICO isomer within 0.2 eV. We also note that the ICO and GM do not normally have the same spin (e.g., ICO Ca_{13} is a septet) and some ICO are strongly distorted (e.g., ICO Mo_{13} has S_{NN}=37 and η=−0.21). Different spin states are sometimes quite close in energy. In that respect, Rh_{13} is remarkable: it has a $2S+1=1$ ground state, a $2S+1=9$ state only 0.08 eV higher in energy, and many other spin states at slightly higher energies, all of them with essentially the same equilibrium structure as shown in Fig. 1. Cadmium is special. The cohesive energies, in eV/at., are 0.18 for the GM in PBE (an ICO which is 0.04 eV below the structure of Fig. 1) and 0.47 for the GM in LSD. The average NN distances (Å) are 3.74 (ICO, PBE), 3.50 (non-ICO, PBE), 3.46 (ICO, LSD), and 3.30 (non-ICO, LSD), while the Cd bulk experimental value is 2.98. Cd_{13} is best described as a nonmetallic van der Waals cluster in PBE, and semimetallic in LSD. We took the ICO Cd_{13} PBE results in all our analyses for consistency but we display the LSD GM in Fig. 1 because it is more metallic and carries additional information.

Some conclusions are immediate from Fig. 1 and the relative energies (REs) and S_{NN} in Tables I and II. First, only 5 elements (Li, Y, Zr, Pd, and Cd) out of 26 have the ICO as their GM, and 2 more (Sr and Mo) have it within 0.1 eV of the GM according to at least one XC functional. Second, the

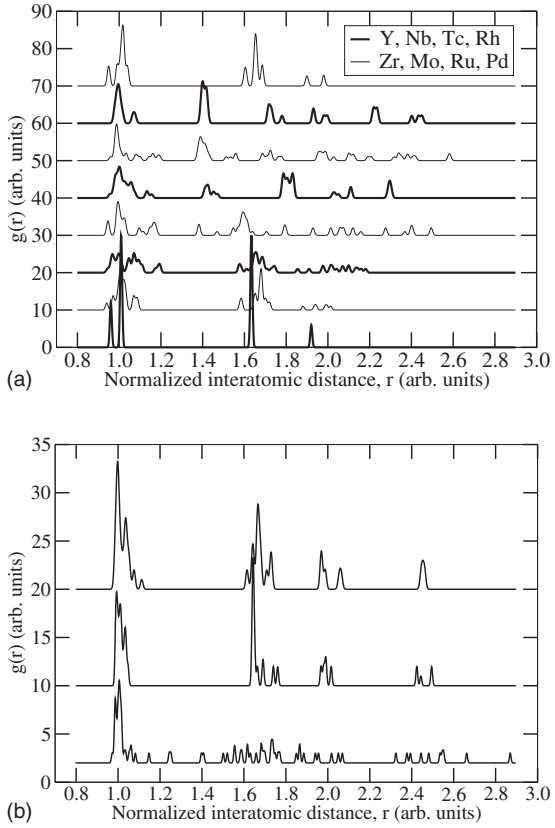

FIG. 2. (a) Normalized pair distribution of second-row transition metal clusters M_{13}, for M=Y (bottom) to M=Pd (top); (b) normalized pair distribution for K_{13} (bottom), Ca_{13}, and Ag_{13} (top).

ICO has a high energy in all of the third-row TM elements (Z=73–78). Third, S_{NN} is a lot smaller than 42 (smaller than 36) in many non-ICO GM. Clearly, surface energy and pair interactions are not sufficient to explain our cluster geometries. This is in striking contrast with empirical potential studies which find essentially the same GM structures, all based on icosahedral growth, for clusters of K, Ca, Rb, Sr, Rh, Pd, and also Na, Ni, and Cs,[7] over a range of nuclearities including n=13.

Some aspects of structure cannot be seen from Fig. 1 or the descriptors in Tables I and II but become apparent in plots of distribution functions. In Fig. 2 we show pair distribution functions $g(r)$ normalized by dividing actual distances by the average of nearest-neighbor distances for that cluster. As expected, the positions of the first peak in those distributions are all very close to r=1 allowing easy comparisons between elements. Distribution functions of second-row TM series clusters, in Fig. 2(a), show that the first peak tends to be wider for clusters near the middle of the TM series. Note that the width of the first peak is larger in Zr_{13} (a distorted ICO) than in Y_{13} (a nearly ideal ICO). A rationale for this trend is that d-type bonding is directional. The extent of d contributions to bonding for atom pairs (i,j) is affected by the angular distribution of neighbors j (and k) around atom i, and there should be important variations in d bonding between (i,j) pairs if angles θ_{jik} differ from 90° (the angle between lobes of d-type functions). This, in turn, gives significant variations in equilibrium interatomic distances for elements near the middle of the TM series that do not have cubic structures. Thus, Ru_{13} and Rh_{13} have relatively narrow first peaks despite important d bonding because of cubic arrangement, but Nb_{13}, Mo_{13}, and Tc_{13} have wide first peaks. Figure 2(b) shows the pair distribution for K, Ca, and Ag. It confirms that, in the absence of d bonding, the first peak is narrow. Pair distributions for the other clusters, not shown here, also follow the trend.

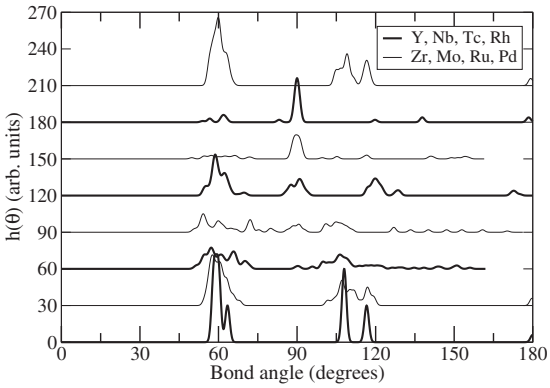

FIG. 3. Bond angle distribution of second-row transition metal clusters M_{13}, for M=Y (bottom) to M=Pd (top).

One can also look at distributions of bond angles $h(\theta)$. For this, we consider only triplets of atoms jik for which (i,j) and (i,k) are neighbors ($d_{ij}<d_0$ and $d_{ik}<d_0$). We show $h(\theta)$ in Fig. 3 for the series Y_{13} to Pd_{13}. Here, as in Fig. 2, one can see that distortions of the ICO increase in the order Y, Pd, and Zr. Among the remaining clusters, Nb_{13} and Mo_{13} have much broader distributions than Tc_{13}, Ru_{13}, and Rh_{13}, consistent with the more amorphous character of their structure.

It is apparent in Fig. 1 that some GM structures are very similar. Recall that the GM of Cd_{13} is an ICO, it is not the structure in Fig. 1. Arranging GMs into subsets of similar geometries would make it easier to identify trends. However, visual inspection can be misleading and give unreliable classifications. Therefore, we quantified similarities between pairs (a,b) of GM structures with a similarity index (SI) $\mathrm{Sim}(a,b)$ calculated on the basis of the distributions of distance $g(r)$ and angles $h(\theta)$. We define two kinds of SIs:

$$\mathrm{Sim}(a,b;r) = \frac{\int g_a(r) g_b(r) dr}{\left[\left(\int g_a(r)^2 dr\right)\left(\int g_b(r)^2 dr\right)\right]^{1/2}}, \quad (6)$$

$$\mathrm{Sim}(a,b;\theta) = \frac{\int h_a(\theta) h_b(\theta) d\theta}{\left[\left(\int h_a(\theta)^2 d\theta\right)\left(\int h_b(\theta)^2\right) d\theta\right]^{1/2}}. \quad (7)$$

TABLE III. Classification of the GM into similarity subsets. Slashes separate less similar elements within a subset.

Li, Y, and Cd/Pd	ICO / Pd is distorted (D_{3d})
Be	Prolate cage
Mg, K, and Zn	Open prolate structure
Al and In	Decahedron
Ca, Rb, Sr, and Ag	Fused pentagonal bipyramids
Zr	Asymmetric, strongly distorted ICO
Nb and Ta	Hexagonal ICO analog minus 2 atoms
Mo and W	Prolate multiply capped trigonal prism
Tc and Re	Biplanar fcc fragment
Rh, Ir/Ru, and Os	Cubic and/or prismatic structure
Pt	Oblate multiply capped trigonal prism

We then used a data clustering algorithm[31] to analyze similarity for each definition of SI, and looked for common features in the resulting classifications. Based on this, we propose to arrange the GMs into the 11 categories shown in Table III. Note that GM belonging to a same category are not identical and sometimes do not even look similar in Fig. 1, for example, K and Mg, or Ca and Sr. So, if we looked into finer details, we could come up with more than 11 categories. However, we think the classification of Table III represents the best compromise. It reveals similarities (for example, between Ca, Rb, Sr, and Ag) that are hidden when structures are represented with ball-and-stick models as in Fig. 1. It also shows that, on the important criteria of interatomic distances and bond angles, the difference between Zr_{13} and other ICO is bigger than, for example, the difference between Sr_{13} and Ag_{13}. The diversity in GM structures is quite remarkable and cannot be accounted for by any simple model or structural principle. For instance, varying the range of the Morse potential in a pairwise additive model produces only two possible GM, the ICO and decahedron (Al_{13} in Fig. 1):[32] 19 of our GM are outside these categories. Notwithstanding the diversity and complexity in GM stuctures, there *are* some periodic trends: most categories in Table III are made of elements that are isovalent or neighbors in the Periodic Table. Further more, we will show that some of these trends can be explained with simple ideas.

The EJM predictions agree with results for only 6 out of 11 elements in Table I (Be, Mg, Al, K, Zn, and In). Obviously, clusters cannot simultaneously maximize S_{NN} and adopt the EJM shape, and that accounts for the non-EJM shape for Li, Cd, and maybe Sr, but it still leaves Rb and Ca looking anomalous. The EJM is not applicable, or does not work, for elements in Table II.

The descriptor RMSD(c) is minimized when all atoms in a cluster have equal coordinations, that is, ring- or cagelike structures. It is large (>1.5) in compact structures like the ICO where interior atoms have a much higher coordination than other atoms. We suggested that larger hardness in atoms correlates with a higher propensity for cagelike cluster structures [smaller RMSD(c)],[18] with hardness defined as half the difference between the energies of the atomic anion and cation, (IE−EA)/2. The argument for this is that increasing RMSD(c) is normally accompanied by increasing partial atomic charges, and there is an energy cost for (hypothetically) charging atoms in a cluster that is proportional to hardness.[33] Beryllium and gold have large hardness compared to other metals and they apparently adopt cage structures in some of their clusters.[5,18] Main group elements have larger hardness and their clusters have smaller RMSD(c) still. In Table IV we give the calculated RMSD(c) of the proposed GM structures along with the hardness of the atoms, (IE−EA)/2, where we used the NIST database[34] experimental values of ionization energies (IEs) and electron affinities (EAs) of the atoms. In cases where the atomic anion is unstable, we used zero as the value for EA. As stated earlier, Cd_{13} is different from the rest in that its low cohesive energy and large interatomic distances indicate nonmetallic bonding. Hence, we treat Cd as a special case in the following analysis. Overall, we find a weak correlation between RMSD(c) and hardness. However, if we partition the 26 elements into two subsets, the *sp* metals without Cd (Li, Be, Mg, Al, K, Ca, Zn, Rb, Sr, Ag, and In), and all the others, we get correlation coefficients of −0.65 and +0.03, respectively. Excluding Cd from the second group changes its correlation coefficient from +0.03 to −0.11. So RMSD(c), and to some extent η, helps us rationalize structures of *sp* metal clusters, but not TM clusters.

It has been noted that squares and cubes, or generally, 90° bond angles (our descriptor R) are present in many TM

TABLE IV. RMSD(c) descriptor of GM and hardness, in eV, of the corresponding atom.

GM	Li	Be	Mg	Al	K	Ca	Zn	Rb	Sr
RMSD(c)	1.60	0.71	1.23	1.93	1.22	1.70	1.15	1.71	1.61
Hardness	2.39	4.66	3.82	2.78	1.92	3.04	4.70	1.85	2.82
GM	Y	Zr	Nb	Mo	Tc	Ru	Rh	Pd	
RMSD(c)	1.60	1.60	1.81	1.32	1.45	0.93	0.93	1.60	
Hardness	2.95	3.10	2.93	3.17	3.19	3.16	3.16	3.89	
GM	Ag	Cd	In	Ta	W	Re	Os	Ir	Pt
RMSD(c)	1.70	1.60	1.88	1.96	1.31	1.45	0.94	0.80	1.54
Hardness	3.14	4.50	2.69	3.78	3.58	3.49	3.68	3.77	3.42

clusters.[15,35,36] We find that R is smallest for elements that bind only through s-type orbitals, and is largest for d-rich TM elements (d_n, $5 \leqslant n \leqslant 8$). The periodic variation of R among TM (Table II) is striking. A rationale for this is that various combinations of p-type and d-type orbitals are mutually perpendicular, and the lobes of d-type orbitals themselves are at 90° of each other. So p-type and d-type bonding interactions should favor the formation of 90° bond angles to maximize orbital overlap. On the other hand, if s-type interactions dominate, bonding is nondirectional and surface area minimization and other effects normally lead to structures with small R like the ICO. Among transition metals, the propensity for large R values is expected to depend, to a first approximation, on $\min\{m_d, 10-m_d\}$, where m_d is the number of d-type electrons in the atom's effective electronic configuration appropriate for a cluster (or solid), typically a $d^{n-1}s^1$ configuration. Furthermore, according to the well-known Slater's rules, the effective screened nuclear charge increases from left to right in a period. Therefore, bonding should take on a more localized character on the right of the TM series. The combination of these two things gives a rationale for why the R values do not peak in the middle of the TM series, but slightly to its right. That is where $\min\{m_d, 10-m_d\}$ is large enough and $d-d$ interactions are relatively more localized. This is a somewhat oversimplified view of course: a detailed rationale of bond angles, insofar as that is possible, would require analysis of orbitals including the role of sd hybridization on a case-by-case basis.[24] The largest contributions to R can be traced back to a few structural motifs: tricapped trigonal prisms in Mg, Zn, Mo, W, and Pt; decahedron (Al and In); octahedra in the fcc fragments (Tc and Re); and of course cubes and prisms (Ru, Rh, Os, and Ir).

IV. SUMMARY AND CONCLUSIONS

We obtained low energy structures for 26 X_{13} metal clusters by DFT and global optimization. We found only a few icosahedra, and much diversity, among structures. There are periodic trends in the calculated GM cluster structures, in the sense that elements belonging to the same similarity category (Table III) are often isovalent or in adjacent columns of the Periodic Table. However, these periodic trends are not simple or strictly obeyed. For example, the first category in Table III (icosahedra) has elements from all over the Periodic Table: this is probably because the driving force that favors ICO formation (surface energy minimization) applies to all elements whereas other aspects of bonding (such as $d-d$ bonding) apply only to some of the elements. We see two correlations between cluster structure and atomic properties: (i) in simple metals RMSD(c) correlates with hardness, and (ii) the presence of 90° bond angles correlates with unfilled valence p- or d-type orbitals. *A posteriori* GM structures seem to be the result of a different balance, for each element, between competing structural principles: maximize S_{NN}, maximize R, minimize RMSD(c), and achieve an optimal shape (η) for a given electron count.

ACKNOWLEDGMENTS

We thank Chi-Kit Siu for his help with computer hardware and VASP software. This work was made possible by the facilities of the Shared Hierarchical Academic Research Computing Network (SHARCNET:www.sharcnet.ca) and support by the Natural Sciences and Engineering Research Council of Canada.

[1] M. B. Knickelbein, Annu. Rev. Phys. Chem. **50**, 79 (1999).
[2] J. A. Alonso, *Structure and Properties of Atomic Nanoclusters* (Imperial College, London, 2005).
[3] R. Fournier, J. Chem. Theory Comput. **3**, 921 (2007).
[4] See, for example, A. Fielicke, C. Ratsch, G. v. Helden, and G. Meijer, J. Chem. Phys. **122**, 091105 (2005), and references therein.
[5] S. Bulusu, L.-S. Wang, and X. C. Zeng, Proc. Natl. Acad. Sci. U.S.A. **103**, 8326 (2006).
[6] W. A. DeHeer, Rev. Mod. Phys. **65**, 611 (1993); M. Brack, *ibid.* **65**, 677 (1993).
[7] M. S. Stave and A. E. DePristo, J. Chem. Phys. **97**, 3386 (1992); J. E. Hearn and R. L. Johnston, *ibid.* **107**, 4674 (1997); G. M. Wang, E. Blaisten-Barojas, A. E. Roitberg, and T. P. Martin, *ibid.* **115**, 3640 (2001); S. K. Lai, P. J. Hsu, K. L. Wu, W. K. Liu, and M. Iwamatsu, *ibid.* **117**, 10715 (2002); B. V. Reddy, S. K. Nayak, S. N. Khanna, B. K. Rao, and P. Jena, Phys. Rev. B **59**, 5214 (1999); J. Rogan, G. Garcia, J. A. Valdivia, W. Orellana, A. H. Romero, R. Ramirez, and M. Kiwi, *ibid.* **72**, 115421 (2005); F. Aguilera-Granja, J. L. Rodríguez-López, K. Michaelian, E. O. Berlanga-Ramírez, and A. Vega, *ibid.* **66**, 224410 (2002); C.-H. Chien, E. Blaisten-Barojas, and M. R. Pederson, J. Chem. Phys. **112**, 2301 (2000).
[8] T. P. Martin, Phys. Rep. **273**, 199 (1996); T. Schenk, D. Holland-Moritz, V. Simonet, R. Bellissent, and D. M. Herlach, Phys. Rev. Lett. **89**, 075507 (2002); W. K. Luo, H. W. Sheng, F. M. Alamgir, J. M. Bai, J. H. He, and E. Ma, *ibid.* **92**, 145502 (2004).
[9] J. Chen and R. Fournier, Theor. Chem. Acc. **112**, 7 (2004).
[10] C. M. Chang and M. Y. Chou, Phys. Rev. Lett. **93**, 133401 (2004).
[11] H. K. Yuan, H. Chen, A. L. Kuang, A. S. Ahmed, and Z. H. Xiong, Phys. Rev. B **75**, 174412 (2007).
[12] M. Pereiro, D. Baldomir, and J. E. Arias, Phys. Rev. A **75**, 063204 (2007).
[13] A. Lyalin, I. A. Solov'yov, A. V. Solov'yov, and W. Greiner, Phys. Rev. A **75**, 053201 (2007).
[14] S. Li, H. Li, J. Liu, X. Xue, Y. Tian, H. He, and Y. Jia, Phys. Rev. B **76**, 045410 (2007).
[15] L. L. Wang and D. D. Johnson, Phys. Rev. B **75**, 235405 (2007).
[16] C. Luo, C. Zhou, J. Wu, T. J. D. Kumar, N. Balakrishnan, R. C. Forrey, and H. Cheng, Int. J. Quantum Chem. **107**, 1632 (2007).
[17] R. Fournier, J. B. Y. Cheng, and A. Wong, J. Chem. Phys. **119**, 9444 (2003).
[18] Y. Sun and R. Fournier, Comput. Let. **1**, 210 (2005).
[19] U. Röthlisberger, W. Andreoni, and P. Gianozzi, J. Chem. Phys. **96**, 1248 (1992).

[20] M. J. Frisch *et al.*, GAUSSIAN03, Revision C.02, Gaussian, Inc., Wallingford, CT, 2004.
[21] J. P. Perdew, K. Burke, and M. Ernzerhof, Phys. Rev. Lett. **77**, 3865 (1996); **78**, 1396(E) (1997).
[22] G. Kresse and J. Furthmüller, Comput. Mater. Sci. **6**, 15 (1996); Phys. Rev. B **54**, 11169 (1996); G. Kresse and J. Hafner, *ibid.* **48**, 13115 (1993).
[23] P. E. Blöchl, Phys. Rev. B **50**, 17953 (1994); G. Kresse and D. Joubert, *ibid.* **59**, 1758 (1999).
[24] L.-L. Wang and D. D. Johnson, J. Phys. Chem. B **109**, 23113 (2005).
[25] R. Fournier, J. Chem. Phys. **115**, 2165 (2001).
[26] A. Lyalin, I. A. Solov'yov, A. V. Solov'yov, and W. Greiner, Phys. Rev. A **67**, 063203 (2003).
[27] J. Rogan G. García, C. Loyola, W. Orellana, R. Ramírez, and M. Kiwi, J. Chem. Phys. **125**, 214708 (2006).
[28] Deng Kaiming, Yang Jinlong, Xiao Chuanyun, and Wang Kelin, Phys. Rev. B **54**, 11907 (1996).
[29] J. W. Mirick, C.-H. Chien, and E. Blaisten-Barojas, Phys. Rev. A **63**, 023202 (2001).
[30] J. Oviedo and R. E. Palmer, J. Chem. Phys. **117**, 9548 (2002).
[31] G. M. Downs and J. M. Barnard, Rev. Comput. Chem. **18**, 1 (2002).
[32] J. P. K. Doye, D. J. Wales, and R. S. Berry, J. Chem. Phys. **103**, 4234 (1995); J. P. K. Doye and D. J. Wales, J. Chem. Soc., Faraday Trans. **93**, 4233 (1997).
[33] W. J. Mortier, S. K. Ghosh, and S. Shankar, J. Am. Chem. Soc. **108**, 4315 (1986).
[34] See http://webbook.nist.gov/chemistry/
[35] W. Zhang, H. Zhao, and L. Wang, J. Phys. Chem. B **108**, 2140 (2004).
[36] Y.-C. Bae, V. Kumar, H. Osanai, and Y. Kawazoe, Phys. Rev. B **72**, 125427 (2005).